

**Muon Spin Rotation Studies Involving Muonium at High pH**

B.W. Ng, J.M. Stadlbauer and D.C. Walker

Department of Chemistry and TRIUMF, University of British Columbia  
Vancouver, B.C., Canada V6T 1Y6**Abstract**

The muon spin rotation method was used to determine the muon yields in concentrated KOH solutions and to evaluate Arrhenius parameters for the reaction of muonium with hydroxyl ions in dilute aqueous solutions. This latter reaction is relatively slow due to a substantial activation energy, yet there is no kinetic isotope effect at room temperature. The kinetics are well represented by the relationship  $\log k_M = 14.38 - 2100(\pm 260)/T$ . The observed enhancement of the diamagnetic muon yield ( $P_D$ ) from 0.62 to 0.79 as the [KOH] was increased from 0 to 20 M can be accounted for in terms of a 'hot-model' mechanism, by allowing  $k_M$  (or the hot fraction) to vary somewhat. The failure of  $P_D$  to reach 1.0 in such concentrated  $\text{OH}^-$  solutions shows that the muons do not all emerge from the epithermal processes of the track as free  $\mu^+$  ions.

(Submitted to Journal of Physical Chemistry)

## Introduction

Hydrated electrons are known to be generated from hydrogen atoms in water at high pH,<sup>1,2</sup> in a reaction whose net effect is one of proton transfer, as in eq. (1)



This reaction has been used to evaluate the  $\text{pK}_a$  of the hydrogen atom<sup>3</sup> and it has some general interest for it demonstrates that H and  $\text{e}_{\text{aq}}^-$  constitute a conjugate acid-base pair.<sup>4</sup> That such a reaction is not merely a quirk of the the unique assimilation of hydronium and hydroxyl ions in water's structure is provided by observations<sup>5,6</sup> that  $\text{OH}^-$  reacts at nearly the same rate with muonium - the light hydrogen isotope with a positive muon rather than a proton as its nucleus.<sup>7,8</sup> This exact correspondence in rates at room temperature obtained by direct observations on muonium by Percival et al.<sup>6</sup> suggests that other bare nuclei may be equivalently accommodated in the water structure, and that muon-transfer can be considered on a par with proton-transfer, even though the muon's initial identity is not forfeited whereas the proton's is.

In order to study the role of muons in high pH water we decided to determine the Arrhenius' parameters of the muonium analogue of reaction (1), and to see what effect very high  $\text{OH}^-$  concentrations would have on the muonium formation process and on the thermalization of muons.

## Experimental

Muonium ( $\mu^+e^-$ , chemical symbol Mu) is an atom formed at the end of muon tracks when a material is bombarded with energetic positive muons. The yield of muonium atoms varies considerably from one material to another. In the case of water, some 38% of the incident muons seem to be formed initially as Mu, with 62% as diamagnetic states, and zero as radicals. However, using the muon spin rotation technique ( $\mu\text{SR}$ ), one can detect only that half of the Mu ensemble with parallel muon and electron spins (the "triplets",  $^3\text{Mu}$ ) and in practice about half of them are 'lost' (probably depolarized<sup>9</sup>) before they can be seen, so one actually observes only about 10% of the muons as Mu. [Half rather than three

quarters appear as triplets because of the spin polarization of the incident muons.]

Details of the  $\mu$ SR technique and its uses are available elsewhere.<sup>7</sup> The incident muons are spin polarized, and the precession of the spins in a transverse field can be monitored through the asymmetric emission of decay positrons. One measures the frequency, amplitude, and relaxation of the precession signals superposed on a lifetime histogram. These provide, respectively, a measure of: the magnetic state of the muon (as controlled by its chemical association), the number of muons which formed into that state, and their rate of reaction or depolarization from that state. For the present aqueous studies, the oscillations are computer-fitted and then plotted as  $A(t)$  against  $t$  as in eq. (2)

$$A(t) = A_D \cos(\omega_D t + \phi_D) + A_M \exp(-\lambda t) \cos(\omega_M t - \phi_M) \quad (2)$$

after removal of the muon decay and background count rate. Examples of raw data and fitted data are provided in Figure 1.  $A$ ,  $\omega$  and  $\phi$  represent the amplitudes, frequencies and initial phases for the diamagnetic (D) and muonium (M) species respectively. Yields are reported as fractions, so that  $P_D = A_D/A_0$  and  $P_M = 2A_M/A_0$ , where  $A_0$  is the total muon amplitude equal to that found in  $CCl_4$  or  $Al$  at  $\omega_D$ .<sup>7</sup>  $\lambda$  is the decay constant of the "triplet" muonium signal. It is increased by the presence of a solute,  $S$ , which reacts chemically with  $Mu$ . A muonium bimolecular rate constant ( $k_M$ ) is determined from the slope of a plot of  $\lambda$  against  $[S]$  or simply from eq. (3)

$$k_M = (\lambda - \lambda_0)/[S] \quad (3)$$

where  $\lambda_0$  is the value of  $\lambda$  in an experiment with  $[S] = 0$ .

These  $\mu$ SR measurements were performed on the M20 beamline at TRIUMF (Tri University Meson Facility on the campus of the University of British Columbia, Vancouver). For the muonium kinetic studies with  $[OH^-] \sim 10^{-2} M$ , a low energy ('surface') muon beam was used with samples held in thin-walled cells and deoxygenated by continuously bubbling with helium.<sup>10</sup> Each solution was maintained at a selected temperature in the range 0 to 100°C by means of a thermostated copper plate in direct contact with the rear wall of the cell. A thermocouple recorded the actual temperature

of the solution in which Mu was formed. Transverse magnetic fields of 8 G were used so that the muonium precession frequency  $\omega_M$  equalled 11 MHz. Most of the  $P_D$  measurements were performed on highly concentrated KOH solutions held in polyethylene cells at room temperature and utilized fields of 80 G, where the muon precession frequency,  $\omega_D$ , was 1.1 MHz.

Analar grade KOH pellets were used in conjunction with doubly distilled deionized water. pH values were checked by titration for the kinetic study. Mole, volume, and mass fractions were evaluated from the measured masses of KOH and  $H_2O$  used to make the solutions in the  $P_D$  studies. In the case of pure KOH, the cell was filled with KOH pellets, where only a minute fraction of the muons would come to rest in the walls of the vessel or in the gas phase. The presence of some carbonate in the surface layer of the pellets exposed to air could be a source of uncertainty in that measurement.

## Results and Discussion

### 1. Muonium reaction with $OH_{aq}^-$

The data for  $\mu SR$  measurement are accumulated over the main spread of muon lifetimes ( $\sim 0.2$  to  $\sim 5 \mu s$ , see Figure 1), so solute concentrations for muonium reactivity studies must be selected to bring  $\lambda^{-1}$  into the most accurate part of that range. One invariably takes two independent histograms using separate positron telescopes for each experiment and averages the values of  $\lambda$  obtained. For each temperature,  $k_M$  was evaluated through eq. (3) using various values of  $[S]$  with the actual  $\lambda_0$  obtained in a separate experiment on pure water at that temperature (as  $\lambda_0$  changes slightly with temperature<sup>11</sup>). The principal results are given in Table I. An Arrhenius plot (based on:  $k_M = Ae^{-E_a/RT}$ ) is shown in Figure 2, with the resulting Arrhenius parameters being given in Table II.

Apparently there is no kinetic isotope effect for this reaction of  $OH^-$  with Mu compared to H at room temperature (see Table II), as noted before.<sup>6</sup> This suggests the reaction mechanism is the same for Mu as for its H analogue, eq. (4),

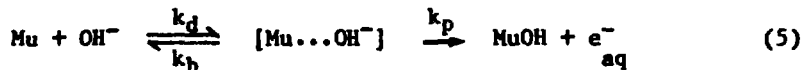


in which the net effect is the transference of a muon to the powerful base:

muonium behaving as a 'muonic acid'.

These reactions of  $\text{OH}^-$  with Mu and H are some three orders of magnitude slower than the diffusion-controlled limit, where  $k_{\text{diff}}$  values of  $\sim 2 \times 10^{10} \text{ M}^{-1}\text{s}^{-1}$  are generally found.<sup>8, 12</sup> Indeed, the observed activation energy of  $40 \text{ kJ mole}^{-1}$  (Table II) greatly exceeds the activation energy for diffusion of species in water, which generally is about  $17 \text{ kJ mole}^{-1}$ .<sup>13, 14</sup> That the reaction is activation controlled is corroborated by the fact that when  $k_{\text{M}}/T$  was plotted against the inverse of the viscosity a pronounced upward curvative was obtained. Had the reaction been diffusion controlled then  $k_{\text{M}}$  would have been proportional to the relative diffusion constants, which in turn would show the temperature dependence of the viscosity (which is not a simple exponential for water<sup>15, 16</sup>).

It is convenient to employ a model such as that depicted in eq. (5)<sup>8, 11, 14</sup>



to describe bimolecular reactions in solution. Hence, the  $[\text{Mu}\dots\text{OH}^-]$  complex is an encounter-pair formed by diffusion (rate constant,  $k_d$ ) and caged momentarily by the solvent. It may yield the reaction product after the first or several "collisions" ( $k_p$ ) or else dissociate by separation ( $k_b$ ). The overall observed rate constant for reaction (4),  $k_{\text{M}}$ , is thus a composite of three parameters, equal to  $k_p k_d / (k_p + k_b)$ . For encounters such as those between Mu and  $\text{OH}^-$  which, evidently, seldom lead to reaction ( $k_b \gg k_p$ ), one has  $k_{\text{M}} \approx k_p k_d / k_b$ . The observed Arrhenius parameters may thus be expected also to be composites:  $A = A_p A_d / A_b$  and  $E_a = E_p + E_d - E_b$ . If one considers the establishment of the encounter-pair as equivalent to a pseudo-equilibrium controlled mainly by diffusive processes, then  $E_d$  and  $E_b$  should be small, and in any event comparable to each other in magnitude. In effect,  $E_a$  approximates  $E_p$ , the activation barrier of the slow rate-controlling step.

With these considerations pertaining to reaction (4), one sees that the muon-transfer step is characterized by an activation energy of  $40 \text{ kJ mole}^{-1}$ . Perhaps this is a measure of the endothermicity of the reaction which may be increased above that of the protium analogue by the increased

zero point energy of the lighter isotope in the transition state and product. This reaction is also associated with an unusually large value of A (see Table II); but, being a composite  $A_p A_d / A_b$ , it may reflect the unique association of  $\text{OH}^-$  with the water structure. Overall, the kinetics of reaction (4) seem to be represented by the relationship:  $\log k_M = 14.38 - 2100(\pm 260)/T$ .

Unfortunately, the Arrhenius parameters for the proton or deuteron analogues [reaction (1)] do not seem to be available for comparison. Contrast may be made with the  $\text{Mu} + \text{HCO}_2^-$  reaction as given in Table II. Here both  $E_a$  and A are smaller than with  $\text{OH}^-$  and there is a large (inverse) isotope effect. Towards formate, Mu is expected to abstract the H-atom - a reaction type in which H is generally more efficient.<sup>8</sup> Certainly, one would not expect formate to be a sufficiently strong base to force Mu to undergo an acid-base transfer as in reaction (4).

## 2. Muon yields in concentrated $\text{OH}^-$ solutions

Because of the foregoing reaction in which  $\text{OH}^-$  converts Mu to the diamagnetic state  $\text{MuOH}$ , one cannot observe muonium directly on the  $\mu\text{SR}$  timescale ( $\sim 10^{-6}$  s) when the pH is greater than  $\sim 12$ . Also, as no Mu-radicals are produced in  $\text{KOH}/\text{H}_2\text{O}$  systems, the only yield that can be observed at very high pH is the diamagnetic fraction,  $P_D$ . This yield was found to change with the mole/mass/volume fractions of  $\text{KOH}$  in the manner shown in Figure 3.  $P_D$  is seen to increase from 0.62 to 0.79 as the medium changed from pure water to ca 50%  $\text{KOH}$ . Solid  $\text{KOH}$  pellets gave a  $P_D$  reading of 0.55.

Equation (2) shows that only those muons with the same initial phase of their spin vectors ( $\phi_D$ ) will precess coherently and thus contribute to the amplitude ( $A_D$ ) of the precession at  $\omega_D$ . Such will be the case for all muons which are initially placed in stable diamagnetic species ( $\mu_{\text{aq}}^+$ ,  $\text{MuOH}$  and  $\text{MuH}$ ) during thermalization in the muon track. It will also include diamagnetic species formed after thermalization; but only in reactions which are sufficiently fast to avoid either dephasing by precession at another frequency or depolarization due to magnetic interactions. Thus, muons which initially appear as muonium atoms must be converted to  $\text{MuOH}$  by chemical reaction with  $\text{OH}^-$  before dephasing or depolarization sets in, if they are to contribute to  $P_D$ . For the muonium atoms with parallel muon

and electron spins (the "triplets",  $^T\text{Mu}$ ) coherence of the muon spin will be largely retained in the product when the reaction rate greatly exceeds the difference between the muonium and muon precession frequencies - which changes with magnetic field. For the "singlets" ( $^S\text{Mu}$ ), however, chemical conversion must precede depolarization of the muon spin by oscillations at the hyperfine frequency,  $\omega_0$ . This is independent of field below the Paschen-Bach region. There is also the possibility of Mu-depolarization leading to 'lost' polarization<sup>17</sup> by encounters with radiation-produced species during the non-homogeneous expansion of the terminal spur<sup>17</sup> or of the entire track.<sup>18</sup>

For the particular case in hand, with  $k_M$  relatively small, almost all the  $^S\text{Mu}$  species will be depolarized at the hyperfine frequency ( $2.8 \times 10^{10} \text{ rad s}^{-1}$ ) because it so greatly exceeds  $k_M[\text{OH}^-]$ , even at 20M ( $3.5 \times 10^8 \text{ s}^{-1}$ ). But dephasing of  $^T\text{Mu}$  at 80 G ( $\omega_M = 6.9 \times 10^8 \text{ rad s}^{-1}$ ) covers the very timescale over which reaction (4) proceeds. One can qualitatively predict, then, that  $P_D$  should increase in these systems from the hot fraction 'h', to a maximum of about  $[h + 0.5(1-h)]$ : i.e. from 0.62 to 0.81, if h remains constant at 0.62.

In this discussion h represents the fraction of muons which form stable diamagnetic chemical states during thermalization - mainly by hot-atom abstraction or substitution reactions during collisional deexcitation following charge exchange, or by thermalization as  $\mu^+$  ions. This use of h has to be distinguished from  $h_D$ , which refers to a much later point in time and was introduced to describe the yield of diamagnetic states emerging from the terminal spur after completion of intraspur reactions, in accordance with the 'spur model' of muonium formation.<sup>17</sup> The value of  $h_D$  changes markedly with the concentration of added scavengers in the range 0.1 to 1 M.<sup>17</sup> But, as all muons emerge from the track thermalized as  $\mu^+$  ions on this spur model, h would necessarily always equal unity. However, the spur model does not seem to be appropriate here, as reaction (6),



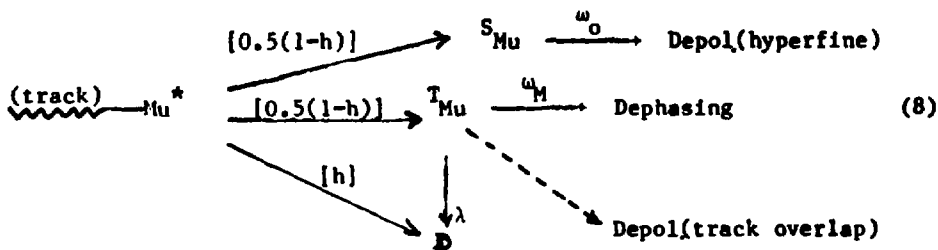
is expected to reduce the lifetime of thermalized  $\mu^+$  to  $< 10^{-12} \text{ s}$  in, say, 10 M KOH, because the proton equivalent of this reaction is one of the fastest known with a rate constant of  $1.4 \times 10^{11} \text{ M}^{-1}\text{s}^{-1}$ .<sup>19</sup> Since spur

reactions in water mainly occur on the timescale  $10^{-11}$  to  $10^{-9}$  s, there is almost no chance for  $\mu^+$  combining with a spur electron to form Mu in the presence of 10 M  $\text{OH}^-$ . Indeed, it was noted previously,<sup>20</sup> that if the spur model applied, the observable muonium yield should have been reduced equally by  $\mu^+$  scavengers as by  $e^-$  scavengers, but no such reduction was found at pH13.<sup>20</sup> The most outstanding feature of Figure 3 is that  $P_D$  does not increase to 1.0. Therefore, we disregard the spur model at this point, for these systems, and continue the discussion in terms of a 'hot model': with  $h$  the initial yield of D and  $1-h$  the initial yield of Mu.

Quantitative treatments have been given for the exact time dependence of the muon polarizations, using various formalisms.<sup>7,21</sup> Following Fleming et al.,<sup>7d</sup> the effective residual polarization is given by eq. (7)

$$P_{\text{res}} = \lim_{t \rightarrow \infty} P(t) \exp(-i\omega_D t) \quad (7)$$

where  $P(t)$  gives the time dependence of the entire muon ensemble including  $T_{\text{Mu}}$  and  $S_{\text{Mu}}$  converted to D. For relatively low fields as here (80 G is only 5% of the hyperfine field, 1585 G), and neglecting the lifting of the muonium degeneracy, one can evaluate the asymmetry seen at frequency  $\omega_D$  based on the model in eq. (8),



where  $\lambda = k_M[\text{OH}^-]$  for reaction (4). Essentially all  $S_{\text{Mu}}$  are depolarized through the hyperfine oscillations before reaction to D as  $\omega_0 \gg \lambda$ , so that half of the Mu ensemble is ignored. Under these conditions, the observed asymmetry will be given by eq. (9),

$$A_D(t) = A_D(0) + A_M(0) \int_0^t \lambda \exp(-(\lambda + i\Delta\omega t')) dt' \quad (9)$$

where  $\Delta\omega = \omega_D - \omega_M \approx -\omega_M$ . Integration of this equation to  $t \rightarrow \infty$  (as in a

μSR experiment)<sup>7d</sup> for the <sup>T</sup>Mu half, followed by normalization to fractional yields, then gives eq. (10):

$$P_D = h + 0.5(1-h)(\lambda^4 + \lambda^2 a_M^2)^{1/2} / (\lambda^2 + a_M^2) . \quad (10)$$

Values of  $P_D$  may be calculated using eq. (10) for comparison with the experimental data of Figure 3. For these high pH systems, in which solute concentrations range from zero to 20 M (up to 0.4 mole fraction), it is highly unlikely that either  $h$  or  $k_M$  (where  $\lambda = k_M[S]$ ) remain invariant; and without independent information as to how they change it is impossible to verify the mechanism of eq. (8) through a fit to eq. (10). Also, there is a further channel by which <sup>T</sup>Mu may be lost [see mechanism of eq. (8)] indicated by depolarization through intra-track encounters of <sup>T</sup>Mu with paramagnetic species, as alluded to earlier. Such encounters are likely to be most important  $\sim 10^{-8}$  s after Mu formation, as the expanding track overlaps with Mu formed some 10 nm beyond it.<sup>18</sup> This extra decay mode will reduce  $P_D$  and is likely to compete with the conversion of Mu → D mainly in the lower portion of the concentration range.

The dashed line in Figure 4 represents a plot of  $P_D$  calculated from eq. (10) by keeping  $h$  and  $k_M$  fixed at their dilute concentration values of 0.62 and  $1.7 \times 10^7 \text{ M}^{-1}\text{s}^{-1}$ , respectively. It differs considerably from the solid line connecting the experimental data. Nevertheless, relatively small variations in  $h$  or  $k_M$  (or both) are required to fit the experimental line. Such data are given in Table III, for allowing  $k_M$  to vary with  $h$  fixed and vice versa. One needs only a four-fold change in the rate constant or an 18% change in  $h$  to fit the data up to 20 M KOH. Such changes are not to be unexpected: so the main point is that the variation in  $P_D$  can be accounted for through the mechanism represented by eqs. (8) and (10), merely by acknowledging that the structural and chemical properties of water change substantially when one third of its molecules are replaced by dissolved KOH. This mechanism is essentially the old 'hot model' of muonium formation, with Mu → D conversion included.

### Acknowledgments

Collaborations with Professor Y.C. Jean and Dr. T.Q. Nguyen during the course of some of these experiments is very much appreciated. Continued financial support through an Intermediate Energy Physics grant from the Natural Sciences and Engineering Council of Canada is gratefully acknowledged.

### References

1. J. Jortner and J. Rabani, J. Amer. Chem. Soc. 83, 4868 (1961).
2. M.S. Matheson and J. Rabani, Radiation Res. 19, 180 (1963).
3. J.H. Baxendale, Radiation Res. Suppl. 4, 139 (1964).
4. (a) D.C. Walker, Quant. Rev. 21, 79 (1967).  
(b) E.J. Hart and M. Anbar in "The Hydrated Electron" (1970), p. 191.
5. (a) E.V. Minaichev, G.G. Myasishcheva, Yu.V. Obukhov, V.S. Roganov, G.I. Savel'ev, V.P. Smilga and V.G. Firsov, Soviet Physics JETP 39, 946 (1974).  
(b) P.W. Percival, E. Roduner, H. Fischer, M. Camani, F.N. Gygax and A. Schenck, Chem. Phys. Lett. 47, 11 (1977).
6. P.W. Percival, E. Roduner and H. Fischer, Ad. Chem. Ser. No. 175, 335 (1979).
7. (a) V.W. Hughes, Annu. Rev. Nucl. Sci. 16, 445 (1966).  
(b) J.H. Brewer, K.M. Crowe, F.N. Gygax and A. Schenck, in "Muon Physics", Vol. III, V.W. Hughes and C.S. Wu, Eds. (Academic Press, New York, 1975) p.3.  
(c) J.H. Brewer and K.M. Crowe, Annu. Rev. Nucl. Part. Sci. 28, 239 (1978).  
(d) D.G. Fleming, D.M. Garner, L.C. Vaz, D.C. Walker, J.H. Brewer and K.M. Crowe, Adv. Chem. Ser., No. 175, 279 (1979).
8. D.C. Walker, J. Phys. Chem. 85, 3960 (1981).
9. P.W. Percival, Hyperfine Int. 8, 325 (1981).
10. Y.C. Jean, J.H. Brewer, D.G. Fleming, D.M. Garner, R.J. Mikula, L.C. Vaz, and D.C. Walker, Chem. Phys. Lett., 57, 293 (1978).
11. B.W. Ng, M.Sc. thesis, University of British Columbia (1980).
12. M. Anbar, Farhataziz, and A.B. Ross, Natl. Stand. Ref. Data Ser., Natl. Bur. Stand., No. 51 (1975).

13. M.J. Pilling, "Reaction Kinetics" (Oxford University Press, London, 1975) p.75.
14. B.W. Ng, Y.C. Jean, Y. Ito, T. Suzuki, J.H. Brewer, D.G. Fleming, and D.C. Walker, J. Phys. Chem. 85, 454 (1981).
15. A.L.F. Lazzarini and E. Lazzarini, J. Inorg. Nucl. Chem. 42, 953 (1980).
16. J.M. Stadlbauer, B.W. Ng, Y.C. Jean and D.C. Walker, J. Phys. Chem. 87, 841 (1983).
17. (a) P.W. Percival, E. Roduner, and H. Fischer, Chem. Phys. 32, 353 (1978).  
(b) P.W. Percival, Hyperfine Int. 8, 315 (1981).
18. D.C. Walker, Hyperfine Int. 8, 329 (1981).
19. M. Eigen and L. DeMaeyer, Z. Elektrochem. 59, 986 (1955).
20. D.C. Walker, Y.C. Jean and D.G. Fleming, J. Chem. Phys. 70, 4534 (1979).
21. (a) V.G. Nosov and I.V. Yakovleva, Soviet Phys. JETP 16, 1236 (1963).  
(b) I.G. Ivanter and V.P. Smilga, Soviet Phys. JETP 27, 301 (1968); 28, 796 (1969); 33, 1070 (1970).  
(c) J.H. Brewer, F.N. Gygax and D.G. Fleming, Phys. Rev. A8, 77 (1973).  
(d) W.R. Fischer, Helv. Phys. Acta 49, 629 (1976).  
(e) P.W. Percival and H. Fischer, Chem. Phys. 16, 89 (1976).  
(f) D.M. Garner, Ph.D. thesis, University of British Columbia (1979).

Table I. Second order rate constants ( $k_M$ ) obtained from  $\lambda$  using eq. (3) at various temperatures and  $\text{OH}^-$  concentrations.

$[\text{OH}^-]/10^{-3}\text{M}$	Temp./°C	$k_M/\text{M}^{-1}\text{s}^{-1}$ <sup>a</sup>
1.60	84	$3.8 \times 10^8$
7.49	59	$1.7 \times 10^8$
49.9	22	$1.7 \times 10^7$
82.5	1	$7.8 \times 10^6$

<sup>a</sup>The overall absolute error in each  $k_M$  value is about 20%.

Table II. Arrhenius parameters obtained for  $k_M$  at ~295 K, and comparison with: (i)  $k_H$ , and (ii) reaction of Mu with  $\text{HCO}_2^-$ .

Reactant	$k_M/\text{M}^{-1}\text{s}^{-1}$	$E_a/\text{kJ mole}^{-1}$	$A/\text{M}^{-1}\text{s}^{-1}$	$k_M/k_H$ <sup>a</sup>
$\text{OH}^-$	$1.7 \times 10^7$	$40 \pm 5$	$(2.4 \pm 0.1) \times 10^{14}$	$1.1 \pm 0.2$
$\text{HCO}_2^-$ <sup>b</sup>	$8 \times 10^6$	$33 \pm 2$	$4 \times 10^{12}$	0.03

<sup>a</sup> $k_H$  values are taken from ref 12.

<sup>b</sup> $\text{HCO}_2^-$  data taken from ref 14.

Table III. Variation of  $k_M$  required for eq. (10) to fit the experimental  $P_D$  data.

$[\text{OH}^-]/\text{M}$	$P_D (\pm 0.01)$	$k_M/10^7 \text{M}^{-1}\text{s}^{-1}$ <sup>a</sup>	$h'$ <sup>b</sup>
0	0.62	1.7	0.62
2	0.62	1.7	0.61
5	0.64	1.7	0.62
10	0.70	3.3	0.66
20	0.79	7.0	0.73

<sup>a</sup> $k_M'$  are the values of  $k_M$  obtained by 'fitting the experimental data to eq. (10), by keeping  $h$  constant at 0.62 but allowing  $k_M$  to change with  $[\text{OH}^-]$ .

<sup>b</sup> $h'$  are the values of  $h$  (hot fractions) necessary to get the 'fitted' solid line if  $k_M$  is invariant at  $1.7 \times 10^7 \text{M}^{-1}\text{s}^{-1}$ .

Figure captions

1. Typical  $\mu$ SR histograms showing the muonium signal at 8 G for (a) pure water at room temperature and (b) its decay in 0.01 M KOH at 60°C. The line drawn is the computer's best fit of the data points to (eq. 2) (see text).
2. Arrhenius plot showing  $\ln k_M$  versus  $T^{-1}$  for the  $Mu + OH^-$  reaction.
3. Variation of  $P_D$  with composition of KOH/H<sub>2</sub>O solutions, plotted as mole ( $\Delta$ ), volume ( ), and mass (•) fractions. The dashed line is the straight line connecting  $P_D$  in pure liquid H<sub>2</sub>O with pure KOH pellets.
4. Plot of  $P_D$  against  $\log [KOH]$ . The dashed line is calculated using eq. (10) with  $h k_M$  constant (see text). The solid line is that used to 'fit' to eq. (10) with  $k_M$  or  $h$  variable - thereby giving the values in Table III.

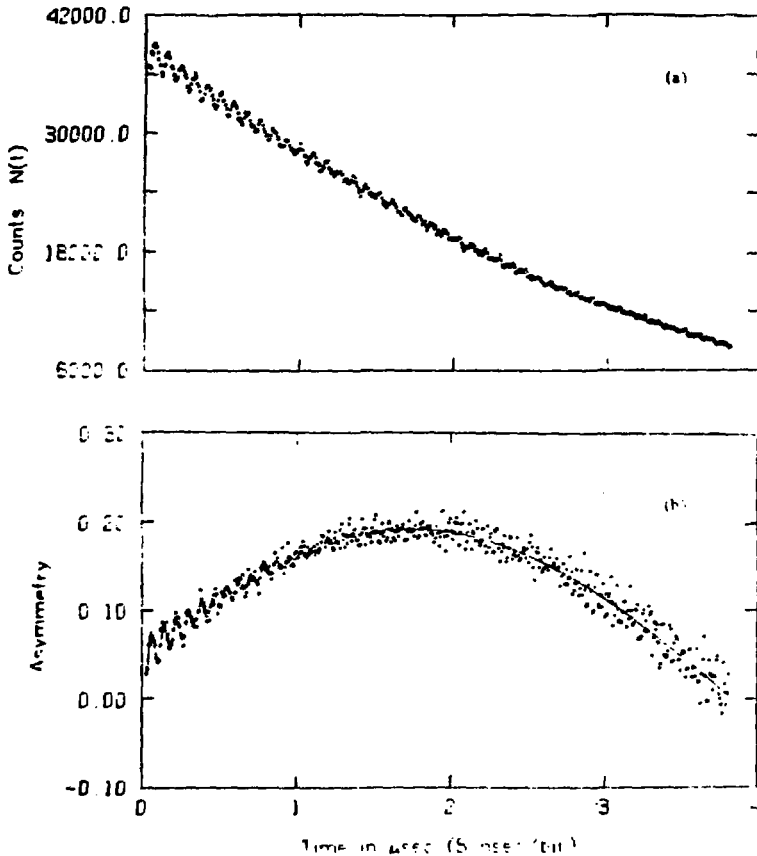


Fig. 1

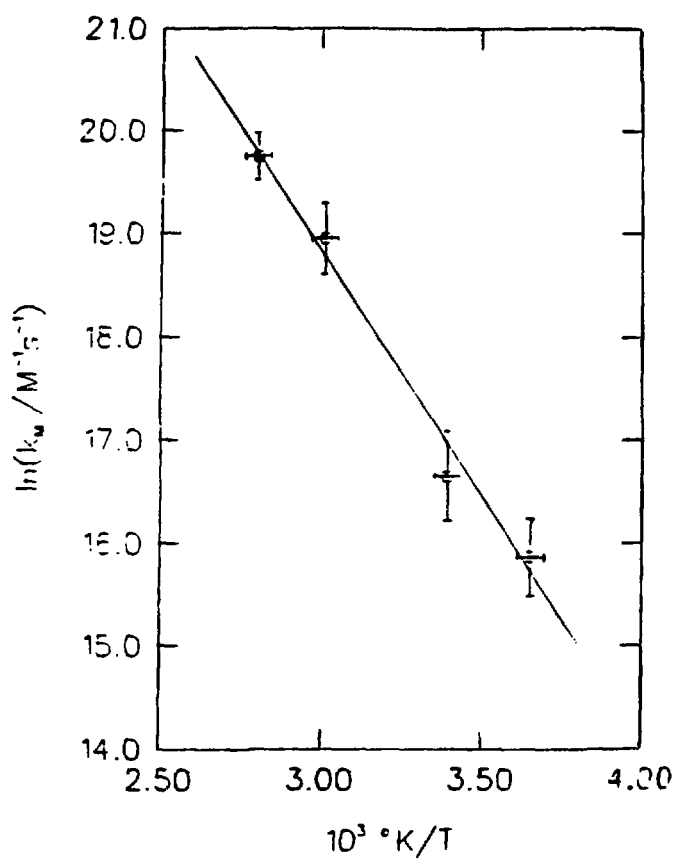


Fig. 2

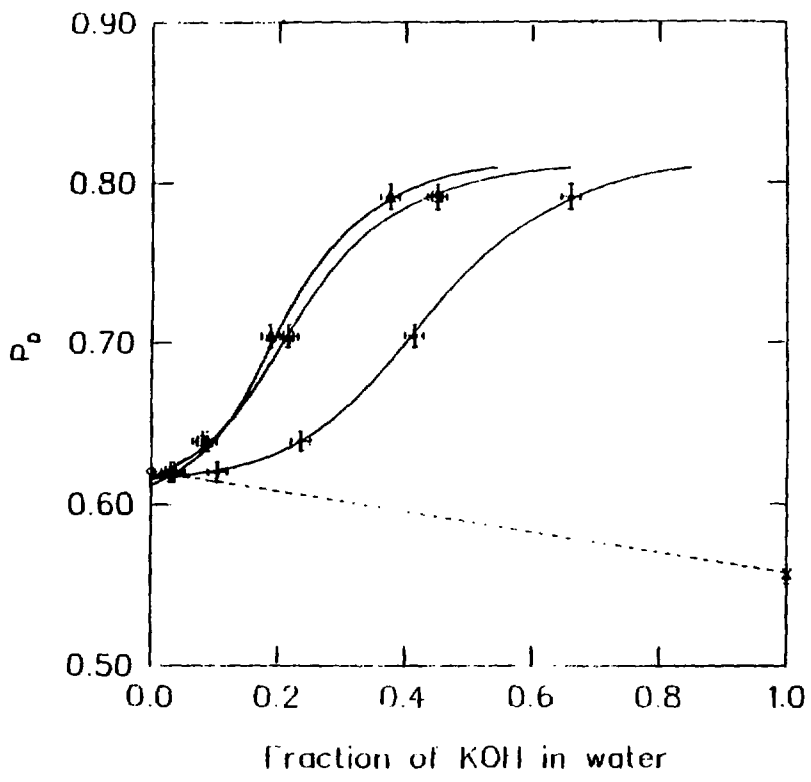


Fig. 3

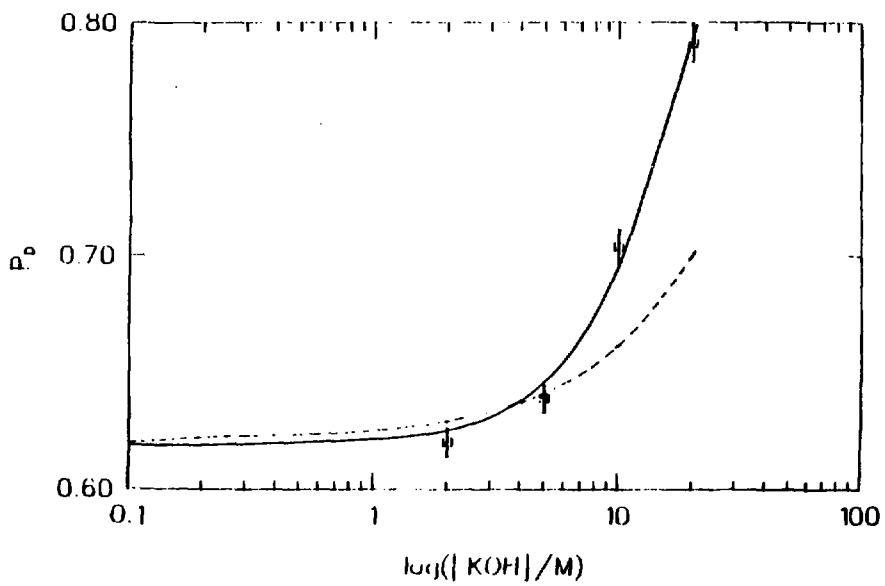


Fig. 4